

## INVESTIGATING MULTIPLE GLARE SOURCES IN DAYLIT CONDITIONS

Quek, Geraldine<sup>1,2</sup>, Yuen, Chui Ling<sup>1</sup>, Wienold, Jan<sup>1</sup>, Andersen, Marilyne<sup>1</sup>

<sup>1</sup>École Polytechnique Fédérale de Lausanne, Lausanne, Switzerland, <sup>2</sup> Singapore University of  
Technology and Design, Singapore, Singapore

geraldine\_quek@sutd.edu.sg

### Abstract

This study explores the effect of multiple bright light sources in the field of view on discomfort due to glare in office environments. User experiments were conducted in semi-controlled dim daylight environments mimicking open-plan offices, with glare stimuli varying in size, number, and position. The findings suggest that being exposed to several bright light sources do not necessarily increase perceived discomfort: a scene with two light sources that were both identified as glare sources by standard detection algorithms was, for instance, perceived less uncomfortable compared to one with a single glare source. This outcome challenges both the current methods of defining/detecting glare sources as well as how the adaptation level is (or should be) accounted for in existing glare metrics. Future research should aim to refine the definition of glare sources and better account for adaptation levels in the presence of multiple sources.

*Keywords:* discomfort glare, metrics, adaptation level, multiple, glare sources, offices

### 1 Introduction

Daylighting in buildings not only serves as an energy-saving, flicker-free source of illumination but plays other vital roles in sustainable building design. With its inherent qualities, exposure to daylight helps regulating humans' circadian rhythms (Cajochen *et al.*, 2005), affecting human health and well-being (Aries, Aarts and van Hoof, 2015; Knoop *et al.*, 2020). By illuminating spaces from the outside, availability of daylight through windows also enables views out, which has been demonstrated to correlate with better productivity, lower stress levels, and higher job satisfaction (Brand *et al.*, 2009; Ko *et al.*, 2017). However, in excess, it can also cause problems such as overheating and discomfort glare, or sometimes lead to privacy concerns, diminishing overall occupant comfort and satisfaction. In the presence of discomfort glare, occupants are likely to resort to closing sun-shading devices, such as roller blinds, to block direct sunlight. A recurrent issue then is that the blinds may thereafter be left closed for the rest of the day, for several weeks or years (Rea, 1984; Maniccia *et al.*, 1999). This results in losing access to daylight and to views out, thereby negating the potential benefits of daylighting and requiring increased reliance on artificial electric lighting. Being able to anticipate discomfort glare risks more reliably in indoor spaces should thus be part of the building design to ensure enough access to daylight while mitigating disturbance to its occupants.

Unlike disability glare, which impairs the vision of objects mostly through intraocular scatter (Stiles and Parsons, 1929), discomfort glare has been defined by the International Commission on Illumination (CIE) as "glare that causes discomfort without necessarily impairing the vision of objects" (CIE, 2011). There are two main phenomena causing discomfort glare: 1) the total amount of light at the eye level and 2) the contrast between adaptation level and glare source. (Hopkinson, Petherbridge and Longmore, 1966). Although Hopkinson and several authors (Iwata and Osterhaus, 2010; Wienold *et al.*, 2019; Quek *et al.*, 2021) used the expression "saturation" for the phenomenon that the perceived discomfort increases when the light level at the eye increases, we decided to call this phenomenon "amount of light at eye level". This expression avoids the impression, that a saturation of any receptor in the eye is causing the discomfort because while the amount of light plays a major role in discomfort glare, the photoreceptors in the eye are still far away from saturation. Glare metrics usually account for one or both phenomena in their equations, with varying performance depending on the prevalent lighting conditions (e.g., bright vs. dim conditions); in those equations, the contrast terms are typically summed up to account for multiple glare sources adding to overall perceived visual discomfort. Depending on the overall adaptation level of the eye, the prediction performance of metrics may vary depending on the type of metric (Quek *et al.*, 2021). Hopkinson's research

suggested that the additivity of glare sources can only be assumed in certain situations (Hopkinson, 1957). It was suggested that in dark or low-light scenes, small glare sources may continue to cause discomfort glare up to a certain luminance threshold, beyond which they no longer contribute significantly to the perceived glare. However, for brighter glare sources, the cumulative effect of multiple sources was suggested to mostly lead to increased discomfort glare. Their later work showed that the cumulative glare effects held true for glare sources with high luminance such as in street lighting applications but not for those with lower luminance (Petherbridge and Hopkinson, 1950). Observers in their experiments adjusted the background luminance to match the perceived level of glare from uncomfortable to imperceptible. Interestingly, the results showed that the perceived glare from two glare sources required less than double the background luminance compared to a single glare source.

In a glare prediction model, Einhorn postulated that, if addition of glare sources is desired, the size of the glare source should be raised to the exponent value of 1, so as to maintain proportionality for the summation of contrast terms from multiple glare sources (Einhorn, 1961). Currently, discomfort glare metrics such as the commonly used Daylight Glare Probability (DGP) and Unified Glare Rating (UGR) sums up the contrast terms of the identified glare sources keeping the size of the glare source raised to an exponent value of 1, and therefore maintain the proportionality. In daylight scenarios, glare sources are usually detected by three methods, that all use a luminance threshold to define which pixel of the image are added to glare sources: 1) using a fixed threshold method of above 2000 cd/m<sup>2</sup> (set as default method in *evalglare* (Wienold, 2004) or 2) The threshold is determined by multiplying luminance of the task area by a factor (default value 5 in *evalglare*) or 3.) The threshold is determined by multiplying the average luminance of the image by a factor (default value 7 in *findglare* (Ward and Shakespeare, 2004)). While previous studies have assessed the influence of glare source detection parameters in *evalglare* on glare metric calculations such as the luminance threshold and search radii (Sarey Khanie *et al.*, 2015; Pierson, Wienold and Bodart, 2018), none have investigated the alignment between these parameters and the actual perceived glare sources by observers. Given the complexities and variations of real office spaces which have generally lower vertical illuminances compared to those studied in controlled laboratory settings (Pierson *et al.*, 2019), the number of glare sources faced by occupants may not be limited to one. Therefore, towards making glare metrics more applicable to real offices spaces, we conducted a user study to investigate the effects of multiple glare sources as well as with the goal of extending the applicability of current glare metrics to low-light conditions (latter goal not part of this manuscript).

## 2 Methodology

We conducted a user study to investigate the effects of multiple glare sources in dim daylight office environments. Although not reported in this paper, the overall scope of the user studies was to investigate discomfort glare responses from users in the luminous range typically encountered in open-plan office spaces in order to extend the validity range of glare prediction models. We used a within-subject, full-factorial experiment design with two independent variables, the position index and size of the glare sources at two levels each. The luminance of the glare source is kept constant in this experiment by maintaining only one level of visible transmittance for the window panels. We modified a room located on the ground floor of a building on the EPFL campus into a dim office space for this study, as shown in Figure 1.

### 2.1 Experiment Setup

Two participants simultaneously participated in the experiment, as shown in position A and B. As shown in Figure 2, the scenes were denoted as “Front-Small”, “Side-Small”, “Front&Side-Small”, and “Center-Large”. Front-small featured a glare source positioned directly above the occupants' line of sight, Side-Small incorporated the same glare source but located at the periphery of the room instead, Front&Side-Small encompassed both aforementioned glare sources, while Center-Large comprised a larger glare source situated in the mid-periphery. For the same scene, each participant experienced the opposite scene of what the other participant experienced – for example, when participant A experiences “Front-Small”, participant B experiences “Side-Small”. As the room is not exactly symmetrically set-up due to practicality, the “Center-Large” scene is not exactly at the same position (even if vertically flipped) for both participants.

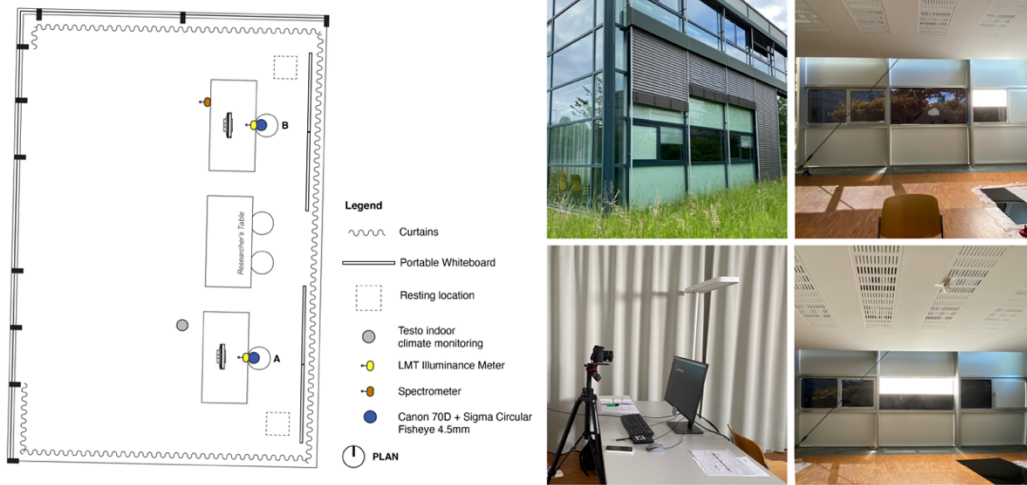


Figure 1 Plan view of the experiment setup in LE Building, EPFL Campus and photos of the experiment setup.

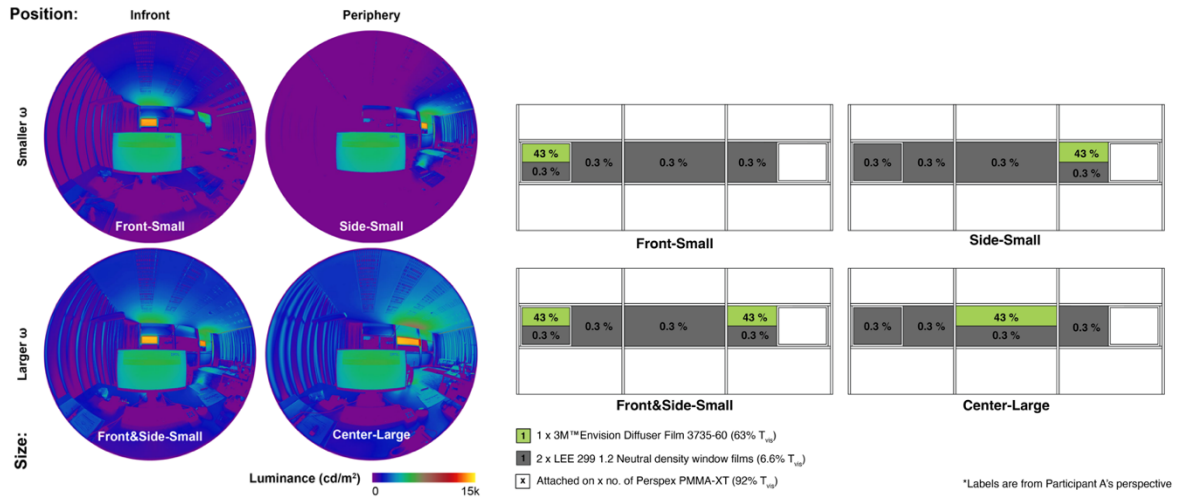


Figure 2 Luminance maps taken using a High Dynamic Range Imager of the four scenes and visual transmittance of window panels for the four scenes, diagrams labelled from the perspective of a participant sitting at position A.

To create the desired low-light levels (Vertical illuminance,  $E_v < 1500$  lux) and high contrasts ( $0.25 < \text{Log}_{gc} < 1.25$ ), four distinct scenes were designed.  $\text{Log}_{gc}$  is the contrast term of the DGP equation, defined in Equation 1. These scenes encompassed variations in the size and position of the glare source, achieved through the utilization of diffuser (3M™ Envision Diffuser Film 3735-60 with a 63% total visible light transmission). To lower the overall illuminance to mimic dimmer open-plan offices, Custom-made 18mm honeycomb cardboard panels were employed to match the dimensions of the window panels and effectively block out daylight for the upper and lower large window panels, which extended over lengths of 2.3 meters.

$$DGP = 5.87 \cdot 10^{-5} E_v + 9.18 \cdot 10^{-2} \underbrace{\log_{10} \left( 1 + \sum_{i=1}^n \frac{L_s^2 \omega_s}{E_v^{1.87} P_i^2} \right)}_{\text{Log}_{gc}} + 0.16 \quad (1)$$

where

- $E_v$  is the vertical illuminance;
- $L_s$  is the luminance of the glare source;
- $\omega_s$  is the solid angle of the glare source;
- $P_i$  is the position index of the glare source.

To keep a reasonable amount of windows providing view to the exterior while minimizing daylight penetration under sunny sky, the remaining middle-band glazing were treated with low-transmission neutral-density films (LEE 299 1.2 with a 6.6% total visible light transmission) attached on Perspex acrylic panels. Existing black-out curtains were opened during the experiment. Figure 2 also shows the final calculated visual transmittances of the façade modified for this user study. The experiment involved the simultaneous control of several environmental parameters to avoid biases or confounding effects. These parameters encompassed maintaining a fixed position for the glare source, ensuring sufficient desktop illuminance, and providing a view to the outside. To maintain thermal comfort, manual interventions were employed, including the use of electric fans and night cooling by opening windows, resulting in temperatures ranging from 24-27°C. Additionally, the experiment necessitated stable weather conditions with a clear sky and direct sun, minimizing cloud cover as much as possible. Given that the room's facade faced west, experiment sessions were conducted during the summer months (May - July) to get optimal sun positions for illuminating the diffuse panels. Each session took place on every available sunny day during this period, from 16:00 to 18:00, following Central European Summer Time (CEST).

## 2.2 Experimental Protocol

The overall 2-hour protocol, as depicted in Figure 3, received approval from the EPFL Human Research Ethics Committee under HREC No. 005-2020 prior to the commencement of the experiment. Participants were compensated for their time. Participants were recruited based on specific prerequisites, including having a minimum proficiency level of at least C1 in English, as defined by the Common European Framework of Reference for Languages (CEFR). They were also required to fall within the age range of 18 to 30 years old and generally have healthy conditions with normal eye health (with the allowance for correction eyewear if needed). After their initial screening, participation was confirmed through email communication. Due to the ongoing COVID-19 pandemic at the time of the experiment, participants were requested to wear a face mask during the entirety of the study to prioritize safety and comply with the recommended health protocols.

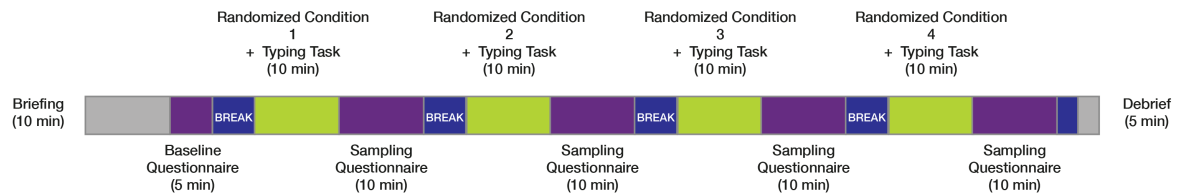


**Figure 3 Experiment protocol used for the user study.**

At the beginning of each session, a brief overview of the experimental procedure was provided. The participant was then introduced to and performed trials of the contrast sensitivity test, Freiburg Visual Acuity Test (FrACT). The height of the high dynamic range (HDR) camera (Technoteam LMK 98-4 colour HighRes and a Dörr Digital Professional DHG fisheye lens) was adjusted to match the participant's eye level. With the external Venetian blinds closed or the black-out curtain drawn, and the electric lighting in the room, the participant completed a baseline questionnaire that collected pseudonymized basic demographic and baseline information, as part of the study design. Following the baseline questionnaire, the participant underwent the FrACT test, which was also administered at the beginning of each sampling questionnaire. The four lighting scenes were presented in a randomized order to both participants. During the breaks between scenes, each participant wore an eye mask and listened to their preferred music through headphones while the researcher adjusted the acrylic panels to prepare for the next scene. After the breaks, the participant visually acclimatized to the scene by engaging in a re-typing task for 10 minutes. Subsequently, the participant completed the FrACT test and a sampling questionnaire on the indoor environmental quality after each scenario administered through the online survey platform, Alchemer. This included six questionnaire items related to discomfort glare presented in a randomized order, including the Glare-indication-diagram (Hirning, Isoardi and Cowling, 2014) and OsterhausBailey-4point (Osterhaus and Bailey, 1992) questionnaire items used for analysis here.

### 2.3 Measurements and data processing

A total of 44 participants were recruited for the experiment and evaluated 4 scenarios each (in total 176 scenes). To ensure the inclusion of only data points with stable weather conditions, gatekeeping conditions were applied to exclude certain data points from the final dataset. The global horizontal irradiation (GHI) obtained from a nearby weather station at a frequency of 1 second was used, and the deviation threshold of 25% was used as a cut-off. These gatekeeping conditions were consistent with those employed by previous researchers (Pierson, 2019). This gatekeeping process resulted in a final dataset comprising 139 data points from 37 unique participants. Glare metrics were then calculated for each of the data points and then subsequently analysed.

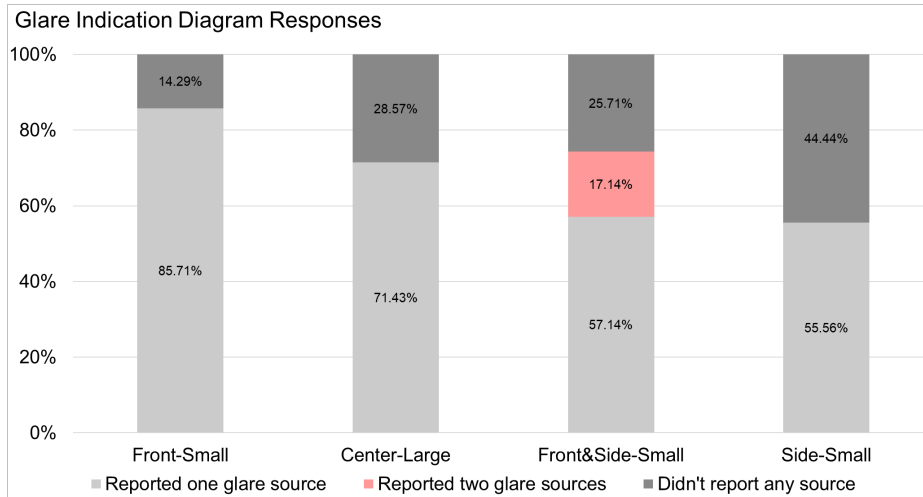
Illuminance data were continuously captured using Hagner SD2 Luxmeters, which were connected to a Hagner multi-channel amplifier (MCA-1600). The amplifier, in turn, was connected to a Keysight data acquisition system (34972A) located in an adjacent room. Handheld vertical illuminance measurements were also taken using a calibrated LMT Pocketlux 2 illuminance meter. Additionally, a spot luminance measurement was obtained using a calibrated Konica Minolta LS100 luminance meter on a grey card. To ensure the spectral qualities of the luminous scene closely resembled daylight, spectral power distribution was measured using the Ocean Insight Jaz spectrometer. Throughout the experiment, thermal comfort was consistently maintained and monitored using the Testo 480 Digital temperature, humidity, and airflow meter. The positions of the measurement equipment for the experiment are indicated accordingly in Figure 1.

To capture high dynamic range (HDR) images, two calibrated Canon 70D cameras were utilized. These cameras were equipped with SIGMA 4.5mm f/2.8 EX DC HSM Circular Fisheye lenses and were placed on stable tripods at the participant's seating position. The cameras were remotely controlled using qDSLR Dashboard to capture a series of 13 exposures, ranging from 1/8000 to 8 seconds. For each exposure, a single image was taken with an aperture of f/11 and the white balance mode set to Daylight. These single exposure images resulted in .jpeg files with dimensions of 5472 x 3648 pixels each. Subsequently, the single exposure images were combined into an .hdr image following Pierson's tutorial (Pierson *et al.*, 2020). The resulting HDR images were then cropped to 3070 x 3070 pixels, corrected for vignetting and geometric distortions, and had the image header adjusted to the lens characteristics. To ensure consistency, all HDR images were individually scaled by custom factors to match the measured spot luminance on the diffuse panel, employing the *pcomb* tool in the Radiance software (Ward and Shakespeare, 2004). Once the HDR images were merged and calibrated, the *evalglare* script was executed on each image using these specific settings: "-b 3000 -r 0.3 -C 0 -d". These *evalglare* settings specified a luminance threshold of 3000 cd/m<sup>2</sup> for detecting glare sources and a search radius of 0.3 radians. The low-light correction was disabled, and a detailed output of the properties of detected glare sources was obtained. The luminance threshold of 3000 cd/m<sup>2</sup> was chosen to ensure the proper detection of all glare sources after manually inspecting the control images and since the luminance of the diffuse panels were above 4000 cd/m<sup>2</sup>. If any "stray" glare sources (any pixel away from the intended glare sources) were identified with less than 1000 pixels, they were re-integrated back into the background luminance. In cases where the HDR images inadvertently captured the computer screen in a dark "screen saver mode" instead of the survey questionnaire window, we manually replaced those pixels with pixels with 115-125 cd/m<sup>2</sup> using a reference HDR image of the same scene type. This post-adjustment was made to ensure consistency and accuracy in the luminance values of the captured images, more specifically for accuracy of the calculated adaptation levels ( $L_b$  or  $E_v$ ).

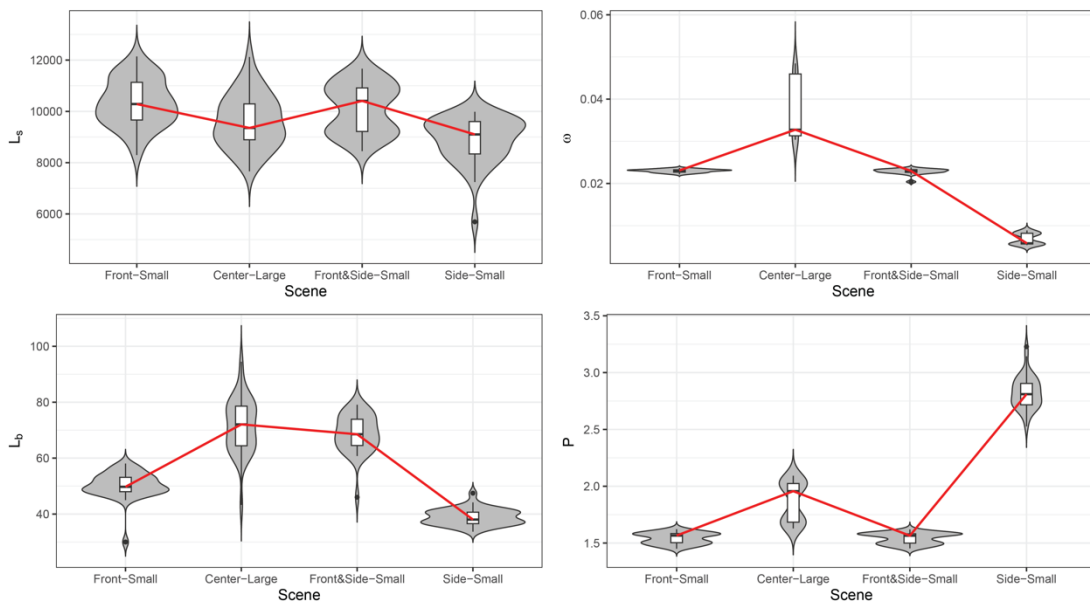
### 3 Results

Figure 4 indicates the result of subjective responses of the glare indication diagram explained in the previous section 2.2 (Figure 5). For Front&Side-Small, the scene with two glare sources, only 17% of participants noted two glare sources while 57% reported one glare source. This may suggest that the second glare source was not perceived as a glare source. Figure 5 shows the descriptive luminous characteristics of the four scenes, namely the luminance of the glare source ( $L_s$ ), the solid angle of the glare source ( $\omega$ ), background luminance ( $L_b$ ) and the position index ( $P$ ). Since majority of participants reported only one glare source for Front&Side-Small (Figure 4), only the characteristics of the glare source that was identified by most subjects is

plot for simplicity (the glare source directly behind the monitor screen). The red lines show the trend of the median statistics of each variable. Figure 6 breaks down the trend of the two terms present in DGP – the vertical illuminance term ( $E_v$ ) and the other term to account for contrast effect (Log\_gc). Comparing the trends between the scenarios, one can observe a similar behaviour between participants' glare responses and Log\_gc, whereas the trend of  $E_v$  does not match user's responses.



**Figure 4 Distribution of Glare Indication Diagram responses for the four scenes.**



**Figure 5 Luminous characteristics of four scenes shown in violin plots. The red trend lines highlight the overall median statistic for each scene. Note: These plots only consider 1 glare source in the scene Front&Side-Small (the glare source directly behind the monitor screen).**

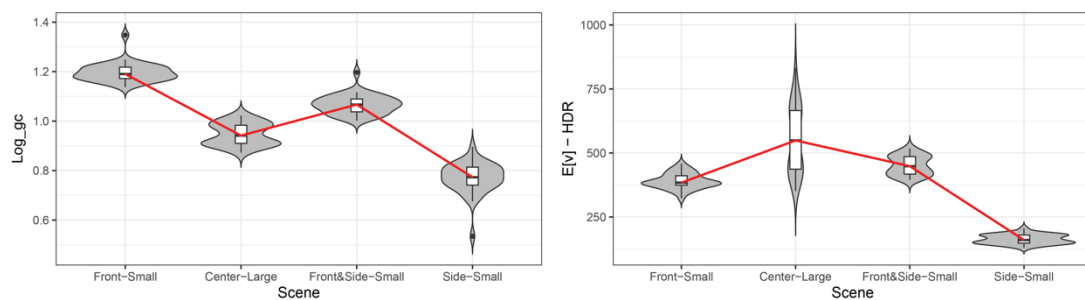


**Figure 6 Violin plots of Log<sub>gc</sub> (contrast term in DGP) and Vertical illuminance (E<sub>v</sub>). Note: These plots only consider 1 glare source in the scene (the glare source directly behind the monitor screen).**

Figure 7 shows the glare responses from the 44 participants who evaluated each scene once. Front-Small, having a glare source right above the monitor screen, had the highest percentage of participants (44%) reporting “Disturbing” when asked how much glare they are experiencing at that moment. The least disturbing scene was the Side-Small scene with a small glare source at the periphery of their field of view with only 2.8% of participants reporting it as disturbing. The Front&Side-Small scene, which was composed of two glare sources had a smaller percentage of disturbing glare reported than the other scenes with one glare sources. Figure 7 also shows the trends of some commonly used glare metrics, DGP, CGI, DGI and UGP/UGR, overlaid on the trend of participants’ glare responses. The median values of metrics in each scene were linearly scaled to match that of Front-Small and Side-Small. The four metrics overestimated the degree of discomfort due to glare in the scene Front&Side-Small compared to Front-Small, using both automatically identified glare sources.

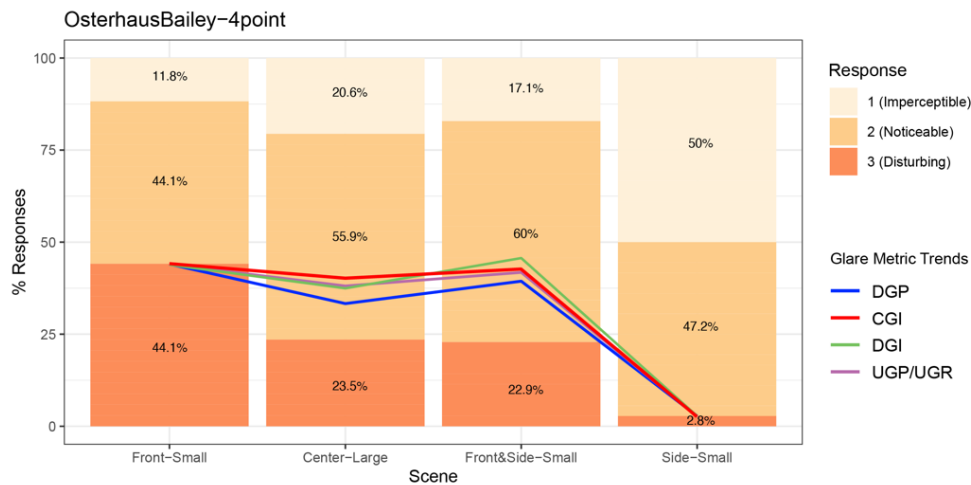


**Figure 7 Glare responses from participants in the four scenes, overlaid with normalized glare metric trends derived from linearly scaling the median values to fit the spread of glare responses from Front-Small to Side-Small. This plot includes both glare sources in Front&Side-Small, as detected by the algorithm.**

## 4 Discussion

Contrary to expectations, the presence of two bright areas in the field of view identified as glare sources each (Front&Side-Small scene) did not result in increased glare reported compared to the Front-Small scene. The presence of a peripheral bright area in this scene appeared to elevate the adaptation level, resulting in a reduced perception of glare, because only 17% of the participants indicated the presence of a second glare source. This opens up an interesting research question: what determines if a bright area is perceived as a glare source?

### 4.1 Glare source definition

What practically defines a glare source requires a more thorough understanding of the respective vs. combined contribution of bright areas to the perception of visual discomfort. In daylight scenarios in particular, where the presence of multiple and inhomogeneous bright areas is very common, this question becomes of high relevance but is also very difficult to answer. Commonly used methods to detect glare sources in HDR images, either implemented in tools such as *evalglare*, *findglare* (Ward and Shakespeare, 2004) or described in published recommendations such as CIE 232:2019 (CIE, 2019) are typically based on luminance thresholds that, for simplicity reasons, do not depend on the location of the bright area(s) in one’s field of view, even though the glare metrics themselves usually include Guth’s position index to account for the positional weighting of glare perception. This simplification, especially when combined to the adaptation level not being accounted for in some of the methods, is thus hypothesized for now as the most convincing explanation of the false detection of glare sources in conditions such as those found in our study. A better understanding of the perceptual

mechanisms involved in how individuals perceive glare sources from future research is essential if we want to establish a clear and consistent definition of a glare source. Such developments would then allow glare source detection algorithms to be improved.

## 4.2 Adaptation level

In scenarios where contrast is the main cause of glare, it is crucial to consider correctly the adaptation level correctly in glare prediction models. DGP and CGI utilize vertical illuminance ( $E_v$ ) to account for eye adaptation. This is a reasonable approach as pupil size is correlated with vertical illuminance through pupil accommodation (Bay *et al.*, 2017). However, the visual system is more complex than just pupil mechanisms accounting for global adaptation. Local adaptation to the visual task and its immediate surrounding may play a role (Sutter, Dumortier and Fontoynt, 2006; CIE, 2019) and is neither considered by  $E_v$  nor by  $L_b$ . Further, it is unclear to what extent glare sources contribute to the adaptation level and may also depend on their size and luminance level. Background luminance,  $L_b$ , (excluding glare sources) is used as a proxy for adaptation level in glare metrics like UGR/UGP, DGI, and PGSV, but was found to be less performant with the dataset where DGP was developed by Wienold (Wienold, 2010). The acquired dataset of this study offers also the opportunity to explore if the usage of  $L_b$  in the DGP equation would better explain the users' perception of glare. For this, we substituted  $E_v$  by  $L_b$  in the contrast term ( $\text{Log}_{gc}$ ) of DGP, but ignored the  $E_v$  term. All exponents for  $L_s$ ,  $\omega$ , and  $P$  were kept the same as in the original formula, for  $L_b$  we inherited the exponent of  $E_v$  of the contrast term (which is 1.87). For the Front&Side-Small scene, only the glare source directly behind the monitor screen was considered as the main glare source and the peripheral glare source was included in the calculation of  $L_b$ .

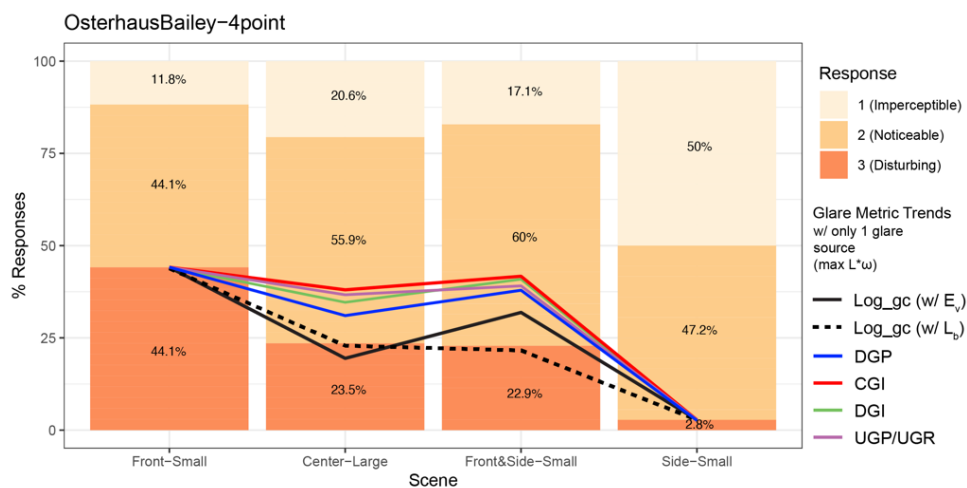


**Figure 8 Comparison between of  $\text{Log}_{gc}$  using background luminance ( $L_b$ ) as the adaptation level, opposed to vertical illuminance ( $E_v$ ), and other glare metrics. (Only one 1 glare source ( $\max L \cdot w$ ) is considered in all calculated metrics in this figure)**

Figure 8 shows that for  $\text{Log}_{gc}$  the trend of the glare responses is better explained using  $L_b$  than  $E_v$  for the adaptation level. This seems to be a promising modification, although the first part of the DGP equation (amount of light at eye level) is ignored for this preliminary investigation. In the same figure the other contrast-driven metrics CGI, DGI, UGP/UGR are also compared to the users' responses. Although they are also calculated using only one glare source they don't match the trend as well as  $\text{Log}_{gc}$  using  $L_b$  for the adaptation level. Given the current limited sample size and range of lighting conditions, further investigations including other lighting scenarios are required to assess the suitability of  $L_b$  to be used as adaptation level when the DGP equation will be extended to levels that are outside the current validity range.

## 5 Conclusion

In conclusion, our user studies highlighted the complex nature of glare perception in daylight environments. More specifically, our evaluation identified two research gaps that need to be investigated in the near future since they impact significantly any glare evaluation for indoor



lighting, for example pertaining to electric light or daylight, or a combination of both. Firstly, existing methods identifying or describing a glare source were shown to be prone to false detection, leading to higher glare metric values and therefore to a mismatch with the participants' responses. We hypothesize that this is caused by the non-consideration of the angular position in the field of view during the detection phase. We further hypothesize that a consideration of a combination of global and local adaptation in the detection phase would be necessary to correctly identify glare sources in the field of view. Secondly, when it comes to the extension of the DGP glare prediction model to levels outside of the current validity range (e.g. for dim daylight environments), the outcomes of the present study show that the nature of the adaptation level, and its underlying mechanisms, should be investigated further before any conclusions can be drawn regarding additivity for instance. Our findings indeed show that for low light scenarios, better predictions could be obtained when  $E_v$  of the contrast term of the DGP equation is replaced by  $L_b$ . In addition, the role of local vs. global adaptation should be further explored as well. Addressing these unresolved issues will enhance the accuracy of discomfort glare predictions and facilitate the development of effective lighting design strategies to enhance visual comfort in indoor office environments.

### Acknowledgements

This research was funded by the Swiss National Science Foundation (SNSF) as part of the ongoing research project, "Visual comfort without borders: Interactions on discomfort glare" (SNSF #182151). Geraldine Quek is a recipient of the Graduate Merit Scholarship from the Singapore University of Technology and Design (SUTD).

### References

- Aries, M., Aarts, M. and van Hoof, J. (2015) 'Daylight and health: A review of the evidence and consequences for the built environment', *Lighting Research & Technology*, 47(1), pp. 6–27. Available at: <https://doi.org/10.1177/1477153513509258>.
- Bay, A. *et al.* (2017) 'COPENHAGEN SEPTEMBER 2017', p. 118.
- Brand, J. *et al.* (2009) 'Linking indoor environment conditions to job satisfaction: a field study AU - Newsham, Guy', *Building Research & Information*, 37(2), pp. 129–147. Available at: <https://doi.org/10.1080/09613210802710298>.
- Cajochen, C. *et al.* (2005) 'High sensitivity of human melatonin, alertness, thermoregulation, and heart rate to short wavelength light', *The Journal of Clinical Endocrinology and Metabolism*, 90(3), pp. 1311–1316. Available at: <https://doi.org/10.1210/jc.2004-0957>.
- CIE (1995) *Discomfort Glare in Interior Lighting*. 117:1995. Vienna, Austria: Commission Internationale de l'Eclairage, p. 41.
- CIE (2011) *ILV: International Lighting Vocabulary*. Standard CIE S 017/E:2011. Vienna, Austria: CIE Central Bureau. Available at: <http://eilmv.cie.co.at/term/17> (Accessed: 10 September 2015).
- CIE (2019) *CIE 232:2019 Discomfort Caused by Glare from Luminaires with a Non-Uniform Source Luminance*. International Commission on Illumination (CIE). Available at: <https://doi.org/10.25039/TR.232.2019>.
- Einhorn, H.D. (1961) 'Pre-Determination of Direct Discomfort Glare', *Transactions of the Illuminating Engineering Society*, 26(4\_IESTrans), pp. 154–164. Available at: <https://doi.org/10.1177/147715356102600402>.
- Hirning, M.B., Isoardi, G.L. and Cowling, I. (2014) 'Discomfort glare in open plan green buildings', *Energy and Buildings*, 70, pp. 427–440. Available at: <https://doi.org/10.1016/j.enbuild.2013.11.053>.
- Hopkinson, R.G. (1957) 'Evaluation of Glare', *Illuminating Engineering*, 52(6), pp. 305–316.
- Hopkinson, R.G., Petherbridge, P. and Longmore, J. (1966) *Daylighting*. Heinemann.
- Iwata, T. and Osterhaus, W. (2010) 'Assessment of Discomfort Glare in Daylit Offices Using Luminance Distribution Images', in: *CIE x035:2010 Lighting Quality & Energy Efficiency*, Vienna, Austria, pp. 174–179.
- Knoop, M. *et al.* (2020) 'Daylight: What makes the difference?', *Lighting Research & Technology*, 52(3), pp. 423–442. Available at: <https://doi.org/10.1177/1477153519869758>.
- Ko, W.H. *et al.* (2017) 'Building envelope impact on human performance and well-being: experimental study on view clarity'. Available at: <https://escholarship.org/uc/item/0gj8h384> (Accessed: 2 March 2022).

Maniccia, D. *et al.* (1999) 'Occupant Use of Manual Lighting Controls in Private Offices', *Journal of the Illuminating Engineering Society*, 28(2), pp. 42–56. Available at: <https://doi.org/10.1080/00994480.1999.10748274>.

Osterhaus, W.K.E. and Bailey, I.L. (1992) 'Large area glare sources and their effect on visual discomfort and visual performance at computer workstations', in *Conference Record of the 1992 IEEE Industry Applications Society Annual Meeting. Conference Record of the 1992 IEEE Industry Applications Society Annual Meeting*, pp. 1825–1829 vol.2. Available at: <https://doi.org/10.1109/IAS.1992.244537>.

Petherbridge, P. and Hopkinson, R.G. (1950) 'Discomfort Glare and the Lighting of Buildings', *Transactions of the Illuminating Engineering Society*, 15(2\_IESTrans), pp. 39–79. Available at: <https://doi.org/10.1177/147715355001500201>.

Pierson, C. *et al.* (2019) 'Discomfort glare cut-off values from field and laboratory studies', in *PROCEEDINGS OF the 29th Quadrennial Session of the CIE. Proceedings of the 29th Quadrennial Session of the CIE*, Washington DC, USA: International Commission on Illumination, CIE, pp. 295–305. Available at: <https://doi.org/10.25039/x46.2019.OP41>.

Pierson, C. (2019) *Discomfort glare perception from daylight: influence of the socio-environmental context*. Université catholique de Louvain.

Pierson, C. *et al.* (2020) 'Tutorial: Luminance Maps for Daylighting Studies from High Dynamic Range Photography', *LEUKOS*, 0(0), pp. 1–30. Available at: <https://doi.org/10.1080/15502724.2019.1684319>.

Pierson, C., Wienold, J. and Bodart, M. (2018) 'Daylight Discomfort Glare Evaluation with Evalglare: Influence of Parameters and Methods on the Accuracy of Discomfort Glare Prediction', *Buildings*, 8(8), p. 94. Available at: <https://doi.org/10.3390/buildings8080094>.

Quek, G. *et al.* (2021) 'Comparing performance of discomfort glare metrics in high and low adaptation levels', *Building and Environment*, 206, p. 108335. Available at: <https://doi.org/10.1016/j.buildenv.2021.108335>.

Rea, M.S. (1984) 'Window blind occlusion: a pilot study', *Building and Environment*, 19(2), pp. 133–137. Available at: [https://doi.org/10.1016/0360-1323\(84\)90038-6](https://doi.org/10.1016/0360-1323(84)90038-6).

Sarey Khanie, M. *et al.* (2015) 'A Sensitivity Analysis on Glare Detection Parameters', in *Building Simulation 2015, IBPSA (Building Simulation)*, pp. 285–292. Available at: <https://doi.org/10.26868/25222708.2015.3024>.

Sørensen, K. (1987) 'A modern glare index method', in *Proceedings of 21st Session of the CIE*, pp. 17–25.

Stiles, W.S. and Parsons, J.H. (1929) 'The scattering theory of the effect of glare on the brightness difference threshold', *Proceedings of the Royal Society of London. Series B, Containing Papers of a Biological Character*, 105(735), pp. 131–146. Available at: <https://doi.org/10.1098/rspb.1929.0033>.

Sutter, Y., Dumortier, D. and Fontoynt, M. (2006) 'The use of shading systems in VDU task offices: A pilot study', *Energy and Buildings*, 38(7), pp. 780–789. Available at: <https://doi.org/10.1016/j.enbuild.2006.03.010>.

Ward, G. and Shakespeare, R. (2004) *Rendering With Radiance: The Art And Science Of Lighting Visualization*. Booksurge Llc.

Wienold, J. (2004) 'Evalglare—A new RADIANCE-based tool to evaluate daylight glare in office spaces', in *3rd International RADIANCE workshop 2004*.

Wienold, J. (2010) *Daylight glare in offices*. Stuttgart: Fraunhofer-Verl.

Wienold, J. *et al.* (2019) 'Cross-validation and robustness of daylight glare metrics', *Lighting Research & Technology*, 51(7), pp. 983–1013. Available at: <https://doi.org/10.1177/1477153519826003>.

Wienold, J. and Christoffersen, J. (2006) 'Evaluation methods and development of a new glare prediction model for daylight environments with the use of CCD cameras', *Energy and Buildings*, 38(7), pp. 743–757. Available at: <https://doi.org/10.1016/j.enbuild.2006.03.017>.